Ac impedance spectroscopy and conductivity studies of $Ba_{0.8}Sr_{0.2}TiO_3$ ceramics

Subrat K. Barik[1], R.N.P. Choudhary[2*], A.K. Singh[3]

[1]*Department of Physics, National Institute of Technology Silchar, Silchar 788010, Assam, India*
[2]*Department of Physics, Institute of Technical Education & Research SOA University, Bhubaneswar 751030, India*
[3]*Department of Physics & Meteorology, IIT Kharagpur, Kharagpur 721302, W.B., India*

[*]Corresponding author. E-mail: crnpfl@gmail.com
.

ABSTRACT

The ac impedance and conductivity properties of $Ba_{0.8}Sr_{0.2}TiO_3$ ceramics in a wide frequency range at different temperatures have been studied. The compound was prepared by a high-temperature solid-state reaction technique. A preliminary structural analysis of the compound by X-ray diffraction technique confirmed its single phase. An ac impedance spectroscopic technique was used to correlate between the microstructure and electrical properties of the compound. The presence of both grain (bulk) and grain boundary effect in the compound was observed. The frequency-dependent electrical data were used to study the conductivity mechanism. An analysis of the electric impedance and modulus with frequency at different temperatures has provided some information to support suggested conduction mechanism. Copyright © 2011 VBRI press.

Subrat K Barik is presently Assistant Professor in Physics at National Institute of Technology Silchar, India. He obtained his M.Sc. from Utkal University (Odisha) and Ph.D. from Vidyasagar University (W.B.) in association with IIT Kharagpur. Later on, he joined at Guru Ghasidas Vishwavidyalaya, Bilaspur. His major field of research is in the area of ferroelectric perovskites. His recent research interest is focused on designing and development of the smart materials for device applications.

R.N.P. Choudhary has worked in National Institute of Technology, Jamshedpur (1971-80) and IIT Kharagpur (1980-2011) as faculty at different levels and positions in physics including head of the department of Physics. During his 40 years of academic career he has made outstanding contributions in research of condensed matter physics including ferroelectrics, liquid crystals, thermoelectrics, multiferroic materials etc for multifunctional applications.

Akhilesh K. Singh is presently a technical staff at IIT Kharagpur. He has obtained his M.Sc. degree in Physics and has been registered for Ph.D. degree in the Vidyasagar University (West Bengal). During his research career, he has prepared and characterized some ferroelectric materials.

Introduction

Some ferroelectric oxides have been the subject of intense research for variety of applications due to their unique ferroelectric, piezoelectric, and pyroelectric properties. Out of the many applications, potential applications of ferroelectric materials are in microwave tunable devices such as tunable mixers, delay lines, filters, and phase shifters for steerable antennas [1-3]. As single crystal of same oxides is difficult to grow at low cost, $(Ba,Sr)TiO_3$ (barium strontium titanate), in ceramic form, has become a leading material system for the above devices due to its high dielectric response and easy tunability near the ferroelectric phase transition temperature T_C [4]. The transition temperature and device parameters of the materials can be controlled by adjusting their compositions. In order to (i) distinguish between grain and grain boundary effects, (ii) make an interpretation of the microscopic processes that allow discerning between dielectric relaxation and long range conductivity processes (i.e., localized and nonlocalized conduction etc.) [5] and (iii) allow distinguishing between the different contributions of the intragrain conductivity, impedance spectroscopy has been widely used in last couple of years, being a powerful technique for the study of the dielectric behavior of crystalline and polycrystalline ceramic materials, especially ionic conductors, ferroelectrics and ferromagnetics [5-8]. Recent works on $Ba_{1-x}Sr_xTiO_3$ (BST) in both bulk and thin films have provided excellent

material properties [9-13]. Detailed literature survey on this material exhibit that no work has been reported on the frequency dependence of electrical (dielectric constant/loss and impedance/conductivity) parameters and to establish correlation between the microstructure and physical properties of the compound. Out of the many compositions of BST, $Ba_{0.8}Sr_{0.2}TiO_3$ possesses a very high degree of structural stability and compositional flexibility due to its ability to accommodate a wide variety of cations on both A and B sites. Further, it is lead free compound on which much attention is now paid. Therefore, we have extensively studied the frequency dependence of dielectric and impedance properties of $Ba_{0.8}Sr_{0.2}TiO_3$ (BST-20) ceramics to get better conduction mechanism in it. In this paper we report our extensive studies on electrical (impedance and conductivity) properties of $Ba_{0.8}Sr_{0.2}TiO_3$ ceramics.

Experimental

Materials preparation

Solid-state reaction technique was used for the preparation of $Ba_{0.8}Sr_{0.2}TiO_3$ (BST-20). High purity ($\geq99.9\%$) ingredients carbonates and oxide; $BaCO_3$, $SrCO_3$ (M/s-Loba Chemie Pvt. Ltd.) and TiO_2 (M/s-S.D. fine-Chem Pvt. Ltd.) were taken in stoichiometric ratios to synthesize BST-20. The precursors were mixed thoroughly using mortar and pestle, first in an air atmosphere for 1.5 h and then in methanol for 1h, so as to make a homogeneous fine powder. Solid-state reaction was carried out in an air atmosphere. The fine powder was calcined at different temperatures/time and finally calcined at optimized temperature/time (1050 ^{0}C, 12 h). The calcined fine powder was cold pressed into circular disc shaped pellet of 10 mm diameter and 1-2 mm of thickness at a pressure of $5x10^6$ N/m^2 using a hydraulic press. Polyvinyl alcohol (PVA) was used as binder which was burnt out during high temperature sintering. These pellets were then sintered at 1080 ^{0}C for 6 h (optimized temperature/time) in an alumina crucible in air atmosphere by slow cooling process. Subsequently, the pellets were polished by a fine emery paper to make their faces smooth and parallel. The pellets were finally coated with conductive silver paint and dried at 150^0 C for 4 h to remove moisture, if any, and then cooled to room temperature before carrying out electrical measurements.

Materials characterization

X-ray diffraction analysis of the calcined powder was studied at room temperature using a diffractometer (Rigaku, Miniflex, Japan) in the range of Bragg angle (20° $\leq 2\theta \leq 80°$) on being irradiated by using CuK_α (1.5405 Å) with a scanning speed of 3^0min^{-1}. The surface morphology or microstructure (i.e., grain size, grain-distribution and voids) of sintered BST-20 sample were recorded by scanning electron microscopy (SEM, JEOL: model JSM-5800F). A pellet sample was gold coated prior to being scanned under high resolution field emission gun of SEM. Electrical impedance (Z), phase angle (θ), tangent loss ($tan\delta$) and capacitance (C_p) were measured as a function of frequency (10^3-10^6 Hz) at different temperatures (31-425 ^{0}C) using a computer-controlled frequency response analyzer (HIOKI LCR HI Tester, Model: 3532) in conjunction with a laboratory-made sample holder and heating arrangement with an ac signal of 1.2V.

Results and discussion

Fig. 1 compares the XRD pattern of calcined $BaTiO_3$ and $Ba_{0.8}Sr_{0.2}TiO_3$ powders at room temperature to confirm the formation of the Sr modified $BaTiO_3$. All the reflection peaks were indexed in different crystal systems and unit cell configurations using a standard computer program package ''POWD'' [14]. Finally, a tetragonal unit cell was selected on the basis of good agreement between observed and calculated interplanar spacing $d[\sum(d_{obs}-d_{cal}) = minimum]$. The XRD pattern confirmed the single phase formation of the compound.

Fig. 1(inset) shows the room temperature scanning electron micrograph of the sintered compound at 5 K magnifications describing their surface property and microstructure. The grains are uniformly distributed throughout the surface of the sample showing its high compactness and polycrystallinity. The density of the ceramics was found to be around 93% of the theoretical density. The average grain size of the compound is ~ 1.3 μm. The presence of voids of irregular dimensions indicates that the sample pellet has certain amount of porosity.
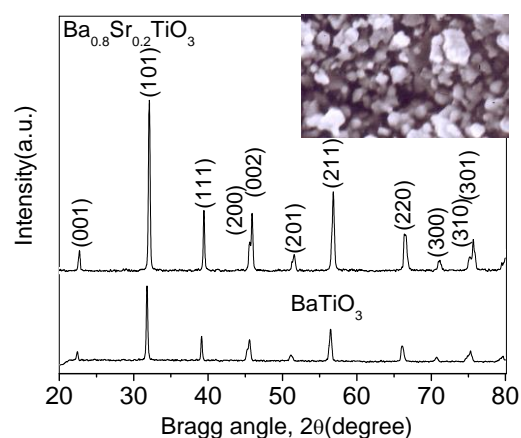
Fig. 1. Room temperature (i) XRD pattern of $BaTiO_3$ and BST-20 and (ii) (Inset) SEM micrograph of the sintered compound.

Fig. 2 shows the frequency dependence of the dielectric constant (ε') and the loss tangent ($tan\delta$) respectively at different temperatures. It is observed that ε' gradually decreases with increasing frequency in a given temperature range. On increasing temperature, ε' increases apparently, which becomes even more significant at low frequency. The decrease in ε' is due to the space charges, which leads to the high dielectric constant and significant frequency dispersion [15, 16]. This indicates the thermally activated nature of the dielectric relaxation of the system [5]. In **Fig. 2**, the loss tangent peak is also found above temperature 250 ^{0}C, and showed a continuous trend of shifting towards high frequencies. The decrease in the value of $tan\delta$ at high

temperatures indicates the presence of dielectric relaxation in BST-20 [**16**].

The electrical behavior of the sample was studied over a wide range of frequency and temperature using a complex impedance spectroscopy (CIS) technique. This technique enables us to separate the real and imaginary components of the complex impedance and related parameters, and hence provides information of the structure-property relationship of the sample. The polycrystalline materials usually have grain and grain boundary properties. Therefore, at high temperatures, two successive semicircles may occur due to these properties. These contributions can conventionally be displayed in a complex plane plots (Nyquist diagram) in terms of the same formalism:

Complex impedance:

$Z^*(\omega)\ (= Z' - jZ'')$

Complex permittivity:

$\varepsilon^*(\omega)\ (= \varepsilon' - j\varepsilon'')$

Complex modulus:

$M^*(\omega)\ (= 1/\varepsilon^*(\omega) = M' + jM'')$

$$tan\delta = \frac{\varepsilon''}{\varepsilon'} = \frac{M''}{M'} = -\frac{Z'}{Z''}$$

where $Z' = |Z|cos\theta$ and $Z'' = |Z|sin\theta$

The frequency dependence of impedance Z'' (loss spectrum) for BST-20 at various temperatures is shown in **Fig. 3**. It is observed that peaks are found at temperature $\geq$ 375 ^{0}C. The position of the Z'' peak shifts to higher frequency side on increasing temperature, and then a strong dispersion of Z'' exists. The width of the peak (**Fig. 3**) points toward the possibility of a distribution of relaxation times [**17**]. In such a situation, one can determine the relaxation time $\tau\ (= 1/\omega_{max})$ from the position of the peak.
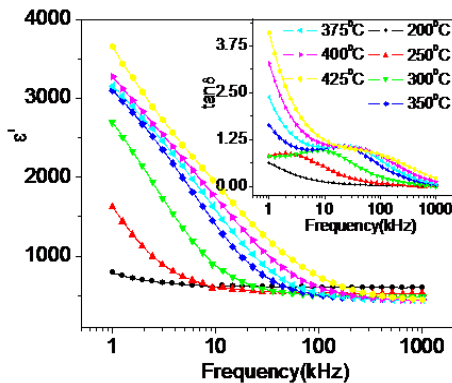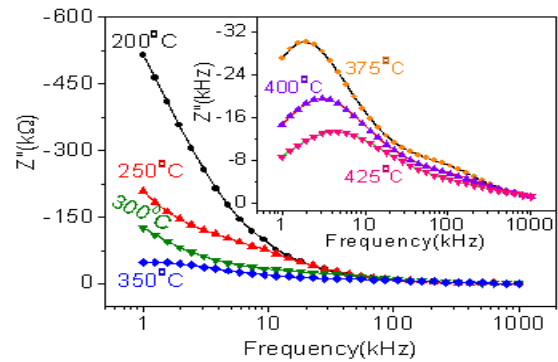
Fig. 3. Frequency dependence of the impedance (Z'') at different temperatures.

Fig. 4 shows a set of Nyquist plots (Z' vs. Z'') over a wide range of frequency (1 kHz - 1 MHz) at different temperatures. The effect of temperature on impedance and related parameters of materials becomes clearly visible with rise in temperature. On increasing temperature, the slope of the lines decreases, and hence they bend towards Z'-axis by which semicircle could be formed. At temperature up to 250 ^{0}C, the absence of second arc in BST-20 confirmed that the polarization mechanism corresponds to the bulk effect arising in semi conductive grains. The intercept of the semicircle on the real axis is the bulk resistance (R_b) of the sample. At higher temperatures ($\geq$250 ^{0}C), it was possible to trace two semicircles [**Fig. 4**]. The appearance of two semicircles suggests the presence of both bulk (grain) as well as grain boundary effects in the studied sample. Each semicircle is a representative of an RC circuit that corresponds to individual component of the material [**18**].

Fig. 4. Nyquist plots (Z' vs. Z'') of BST-20 at different temperatures.

Fig. 5 shows the dc conductivity (σ_{dc}) vs. $10^3/T$ plot of BST-20 at different temperatures. It indicates a pattern in which conductivity increases gradually with rise in temperature suggesting a thermally activated process in the materials [**19**]. The value of dc bulk conductivity has been calculated from the impedance data using the relation, $\sigma_{dc} = t/R_bA$, where R_b is the bulk resistance, t is the thickness, and A is the area of the electrode deposited on the sample.
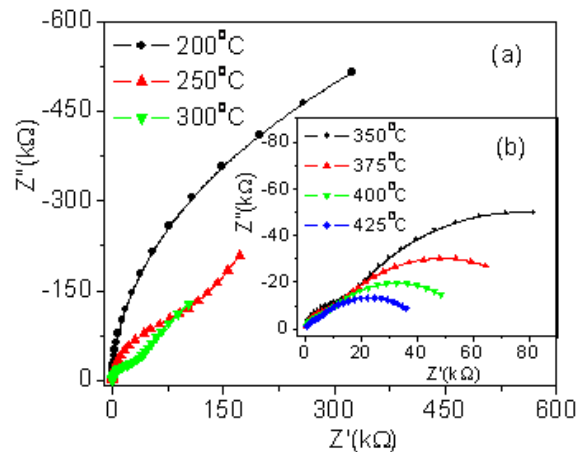
Fig. 2. Frequency dependence of the dielectric constant (ε') and the loss tangent (tan δ) at different temperatures.

Fig. 5(inset) shows the temperature variation of grain boundary conductivity (σ_{gb}). Both the dc bulk and grain boundary conductivity graphs follow the Arrhenius law, and the activation energies evaluated from the slope of the linear portion of the plots are 0.55 and 0.56 eV respectively.

We have adopted the impedance as well as the modulus formalism to study the relaxation mechanism in BST-20. Here the imaginary impedance (Z'') and modulus (M'') are plotted as a function of frequency. The peak is observed in these plots corresponding to a relaxation process. The peak height in Z'' against frequency plot is proportional to the resistance of that process, while the peak height in M'' against frequency plot is inversely proportional to the capacitance.
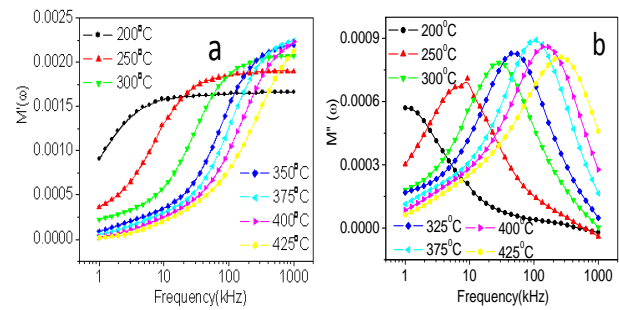
Fig. 6(a-b) show the frequency dependence of dielectric modulus (M' and M'') over a wide range of frequency at different temperatures. Here M' shows a dispersion tending toward M_∞ (the asymptotic value of M' at higher frequencies (**Fig. 6**(a)), while M'' exhibits a maximum M''_{max} which shifts to higher frequencies with increase in temperature (**Fig. 6**(b)). The frequency region below peak maximum M'' determines the range in which charge carriers are mobile on long distances. At frequency above peak maximum M'', the carriers are confined to potential wells, being mobile on short distances. The frequency ω_{max} (corresponding to M''_{max}) gives the relaxation time τ from the condition $\omega_{max}\tau = 1$.
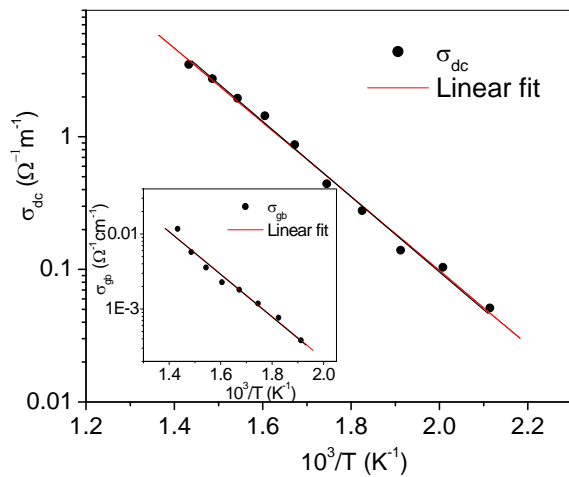

Fig. 5 Variation of dc conductivity and grain boundary conductivity (inset) as a function of temperature.

Fig. 7 shows the modulus master curve of the sample at various temperatures. The capacitance values are calculated at the maximum frequency (f_{max}) using the relation $M'' = \varepsilon_0/2C$. The modulus peak maximum shifts to higher frequencies as temperature increases but the shape and full-width at half-maximum (FWHM) of M''/M''_{max} vs. f/f_{max} do not change in the temperature range considered. The overlap of the curves for all the temperatures indicates that the dynamical processes are nearly temperature independent [20]. It is also observed that the M''/M''_{max} curves are not symmetric, implying a non-exponential behavior of the conductivity relaxation. The FWHM of the

M''/M''_{max} spectra is wider than the breath of a Debye peak (1.14 decade), which suggests the presence of non-Debye type of relaxation phenomenon [19].

Fig. 6. Frequency dependence of (a) imaginary part of dielectric modulus (M'') and (b) real part of dielectric modulus (M') at different temperatures.
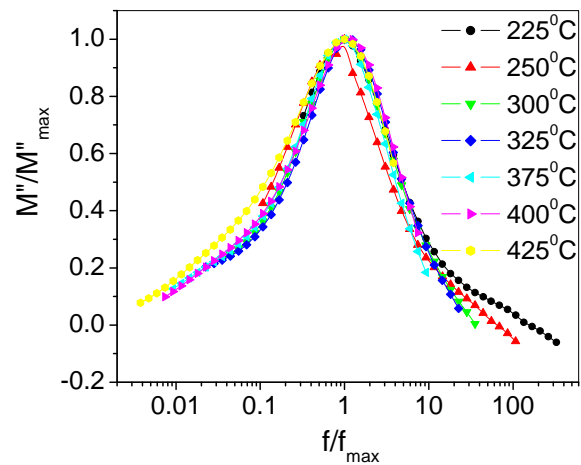

Fig. 7. Scaling behavior of dielectric modulus (i.e., M''/M''_{max} vs. f/f_{max}) and master curve of BST-20 at different temperatures.
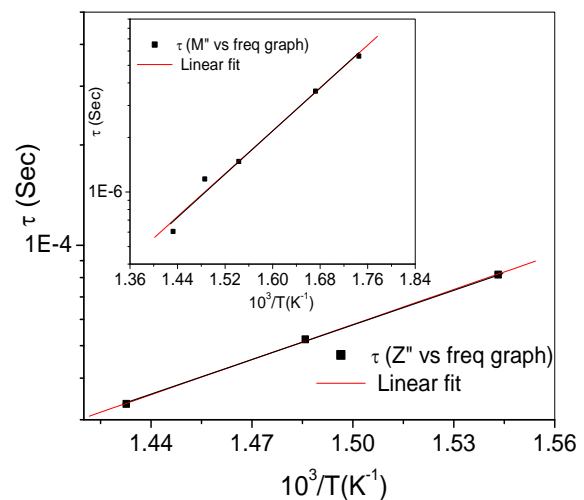
Fig. 8. Variation of relaxation time (calculated from impedance and modulus plot) with temperature.

Fig. 8 shows the variation of relaxation time (calculated from loss and modulus spectrum) as a function of temperature. The relaxation time in both the cases follows the Arrhenius law given by $\tau = \tau_0 \exp (E_a/K_B T)$ where τ_0 is the pre-exponential factor, K_B is the Boltzmann constant and E_a is the activation energy. The typical pattern suggests a temperature dependent relaxation process with spread of relaxation time in the range of 10^{-7}-10^{-5} sec suggesting enhancement in the process dynamics (i.e., charge/carrier transport) in the material with rise in temperature [**21**]. Fitting of these data to Arrhenius equation yields the activation energy E_a as 0.70 and 0.59 eV respectively. The small difference in activation energy calculated from relaxation and conductivity studies suggests that both the process may be attributed to the same type of charge carriers.

Fig. 9 shows the frequency dependence of ac conductivity (σ_{ac}) at different temperatures. At lower temperatures, low frequency plateau and high frequency dispersion of conductivity appear to be observed. Above 250 ^{0}C, a significant change in the conductivity pattern occurs with rise in temperature. In this temperature range, a broader plateau region is observed in the low frequency region and a dispersive behavior of conductivity spectrum appears in the high frequency region irrespective of temperature. The hopping frequency (ω_p) occurs at the point where the slope changes in the conductivity spectrum. The frequency dependent conductivity of the material follows the Jonscher's law [**22**]; $\sigma_{ac} = \sigma_{dc} + A\omega^n$, where n is the frequency exponent in the range of $0 \leq n \leq 1$. It is confirmed by a typical fit of the above equation to the experimental data (shown in figure). The estimated value of n is 0.55. The conductivity behavior (Fig. 9) is governed by a relation; $\sigma \propto \omega^n$ for all temperatures ($\geq$250 ^{0}C). The plateau region corresponds to the frequency independent dc conductivity (i.e., σ_{dc}) and dispersive region corresponds to the frequency dependent part. Further, a rise in the value of conductivity with temperature indicates that the electrical conduction in the material is a thermally activated process.
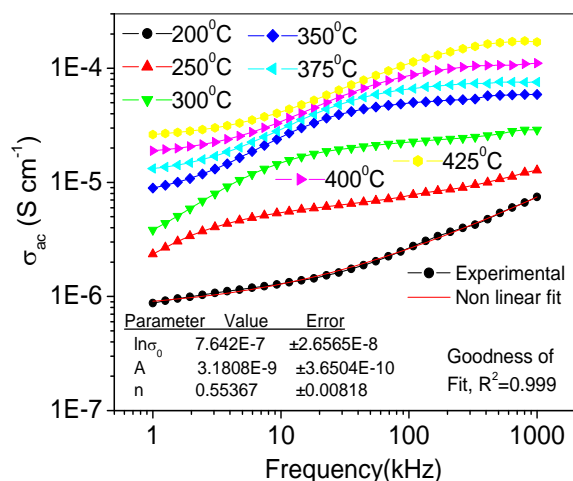
Fig. 9. Frequency variation of ac conductivity (σ_{ac}) at different temperatures.

Conclusion

The frequency-dependent dielectric dispersion of $Ba_{0.8}Sr_{0.2}TiO_3$ prepared by the solid-state reaction technique has been studied. The phase formation of the sample is confirmed by XRD technique. The presence of space charge polarization at higher temperature arises only due to the mobility of ions and imperfections in the material. A better correlation and understanding of the sample electrical properties with its microstructure in terms of bulk and grain-boundary contribution have been described. Dc conductivity (σ_{dc}) shows typical Arrhenius behavior when observed as a function of temperature. The frequency dependence of normalized M and Z shows that all dynamic processes occurring at different frequencies exhibit the same thermal activation process. Modulus analysis has been carried out to understand the mechanism of electrical transport process and this indicates non-Debye type conductivity relaxation in the material.

Reference

1. Lancaster, M.J.; Powell, J.; Porch, A. *Supercond. Sci. Technol.* **1998**, **11**, 1323.
   DOI: 10.1088/0953-2048/11/11/021
2. Tagantsev, A.K.; Sherman, V.O.; Astafiev, K.F.; Venkatesh, J.; Setter, N. *J. Electroceram.* **2003**, *11*, 5.
   DOI: 10.1023/B:JECR.0000015661.81386.e6
3. Yadav, K. L. *Adv. Mat. Lett.* **2010**, *1(3)*, 259.
   DOI: 10.5185/amlett.2010.9159
4. Bao, P.; Jackson, T.J.; Wang, X.; Lancaster, M.J. *J. Phys. D* **2008**, *41*, 063001.
   DOI: 10.1088/0022-3727/41/6/063001
5. Gerhardt R. *J. Phys. Chem. Solids* **1994**, *55*, 1491.
   DOI: 10.1016/0022-3697(94)90575-4
6. James, A.R.; Priya, S.; Uchino, K.; Srinivas K. *J. Appl. Phys.* **2001**, *90*, 3504. **DOI:**10.1063/1.1401802
7. Rai, A.K.; Rao K.N.; Kumar, L.V.; Mandal K.D. *J. Alloys Comp.* **2009**, *475*, 316.
   DOI: 10.1016/j.jallcom.2008.07.038
8. Kumar, Pritam; Singh, B.P.; Sinha, T.P.; Singh, N.K. *Adv. Mat. Lett.* **2011**, *2(1)*, 76.
   DOI: 10.5185/amlett.2010.11176
9. Bellotti, J.; Akdogan, E.K.; Safari, A.; Chang, W.; Kirchoefer, S. *Integr. Ferroelectr.* **2002**, *49*, 113.
10. Lu, S.G.; Zhu, X.H.; Mak, C.L.; Wong, K.H.; Chan, H.L.W.; Choy, C.L. *Appl. Phys. Lett.* **2003**, *82*, 2877.
    DOI:10.1063/1.1569427
11. Jain, M.; Majumder, S.B.; Katiyar, R.S.; Bhalla, A.S.; Miranda, F.A.; Van Keuls, F.W. *Appl. Phys. A: Mater. Sci. Process.* **2005**, *80*, 645.
    DOI: 10.1007/s00339-003-2268-4
12. Ianculescu, A.; Berger, D.; Viviani, M.; Ciomaga, C.E.; Mitoseriu, L.; Vasile, E.; Drăgan, N.; Crişane, D. *J. Euro. Ceram. Soc.* **2007**, *27*, 3655.
    DOI: 10.1016/j.jeurceramsoc.2007.02.017
13. Sigman, J.; Clem, P.G.; Nordquist, C.D.; Richardson, J.J.; Dawley, J.T. *J. Appl. Phys.* **2007**, *102*, 054106.
    DOI: 10.1063/1.2775922
14. Wu E. POWDMULT: An Interactive Powder Diffraction Data Interpretation and Indexing Program, Version 2.1; School of Physical Sciences, Flinder University of South Australia: Bardford Park, SA, Australia, **1989**.
15. Singh, N. K.; Kumar, P.; Kumar, H.; Rai, R. *Adv. Mat. Lett.* **2010**, *1(1)*, 79.
    DOI: 10.5185/amlett.2010.3102
16. Tareev, B. Physics of Dielectric Materials; Mir Publishers: Moscow, **1979**.
17. Macdonald, J.R. Impedance Spectroscopy, Ed.; Wiley: New York, **1987**.

18. Boukamp, B.A. Equivalent Circuit-EQUIVCRT Program Users' Manual, University of Twente, The Netherlands, **1989**; Vol. 3.
19. Barik, S.K.; Choudhary, R.N.P.; Mahapatra, P.K. *Appl. Phys. A* **2007**, *88*, 217.
    DOI: 10.1007/s00339-007-3990-0
20. Padmasree, K.P.; Kanchan, D.K.; Kulkarni, A.R. Solid State Ionics 2006, 177, 475.
    DOI: 10.1016/j.ssi.2005.12.019
21. Victor, P.; Bhattacharyya, S.; Krupanidhi, S.B. *J. Appl. Phys.* **2003**, *94*, 5135.
    DOI:10.1063/1.1606509
22. Jonscher, A.K. *Nature* **1977**, *267*, 673.
    DOI: 10.1038/267673a0

ADVANCED MATERIALS *Letters*

Publish your article in this journal

ADVANCED MATERIALS Letters is an international journal published quarterly. The journal is intended to provide top-quality peer-reviewed research papers in the fascinating field of materials science particularly in the area of structure, synthesis and processing, characterization, advanced-state properties, and applications of materials. All articles are indexed on various databases including DOAJ and are available for download for free. The manuscript management system is completely electronic and has fast and fair peer-review process. The journal includes review articles, research articles, notes, letter to editor and short communications.